

5-8-2017

Catalytic Acceptorless Dehydrogenation of Amines with $\text{Ru}(\text{P}^{\text{R}}_2\text{N}^{\text{R}'_2})$ and $\text{Ru}(\text{dppp})$ Complexes

James M. Stubbs
The University of Western Ontario

Richard J. Hazlehurst
The University of Western Ontario

Paul D. Boyle
The University of Western Ontario

Johanna M. Blacquiere
The University of Western Ontario, jblacqu2@uwo.ca

Follow this and additional works at: <https://ir.lib.uwo.ca/chempub>

 Part of the [Chemistry Commons](#)

Citation of this paper:

Stubbs, James M.; Hazlehurst, Richard J.; Boyle, Paul D.; and Blacquiere, Johanna M., "Catalytic Acceptorless Dehydrogenation of Amines with $\text{Ru}(\text{P}^{\text{R}}_2\text{N}^{\text{R}'_2})$ and $\text{Ru}(\text{dppp})$ Complexes" (2017). *Chemistry Publications*. 178.
<https://ir.lib.uwo.ca/chempub/178>

Catalytic Acceptorless Dehydrogenation of Amines with Ru(P^R₂N^{R'}₂) and Ru(dppp) Complexes

James M. Stubbs, Richard J. Hazlehurst, Paul D. Boyle and Johanna M. Blacquiere*

Department of Chemistry, University of Western Ontario, London, Ontario, N6A 5B7

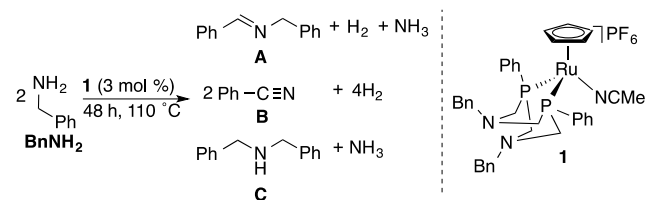
Supporting Information Placeholder

ABSTRACT: [Ru(Cp)(P^{Ph}₂N^{Bn}₂)(MeCN)]PF₆ (**1**; P^{Ph}₂N^{Bn}₂ = 1,5-benzyl-3,7-phenyl-1,5-diaza-3,7-diphosphacyclooctane) and [Ru(Cp)(dppp)(MeCN)]PF₆ (**2**; dppp = 1,3-bis(diphenylphosphino)propane) are both active toward the acceptorless dehydrogenation of benzylamine (BnNH₂) and *N*-heterocycles. The two catalysts have similar activity, but different selectivity for dehydrogenation products. Independent synthesis of a [Ru(Cp)(P^{Ph}₂N^{Bn}₂)(NH₂Bn)]PF₆ adduct (**3**) reveals the presence of a hydrogen bond between the bound amine and the pendent base of the P^{Ph}₂N^{Bn}₂ ligand. Preliminary mechanistic studies reveal the benzylamine adduct is not an on-cycle catalyst intermediate.

INTRODUCTION

Acceptorless dehydrogenation (AD) and acceptorless dehydrogenative coupling (ADC) have recently emerged as atom economic routes to versatile functionalities such as aldehydes, esters, carboxylic acids, amides, imines and amines.¹ Generally, these reactions involve dehydrogenation of an alcohol moiety, typically followed by nucleophilic attack by another alcohol or amine molecule. Relatively few catalysts have been reported for amine dehydrogenation,² but the reaction represents a low-waste synthesis of imines that is an alternative to common oxidative strategies.³ Additionally, release of chemically stored H₂ from amines to give nitriles is desirable for alternative fuel applications.⁴ One of the more successful systems for acceptorless dehydrogenation is the pincer catalysts developed by Milstein.^{1b, 5} This system operates through a cooperative⁶ H₂ removal mechanism that involves proton transfer to the ligand and hydride transfer to the metal.⁷ The success of such a catalyst inspired us to test the established⁸ cooperative P^R₂N^{R'}₂ (1,5-R'-3,7-R-1,5-diaza-3,7-diphosphacyclooctane) ligand family. Similar to dehydrogenation, electrocatalytic H₂ formation (and the reverse H₂ oxidation) is promoted with a number of Ni, Fe and Ru complexes, where the pendent amine of the P^R₂N^{R'}₂ ligand acts as an intramolecular base to shuttle protons to/from the metal.⁹ Herein, we evaluate the catalytic performance toward amine dehydrogenation and preliminary mechanistic details of the known⁹ [Ru(Cp)(P^{Ph}₂N^{Bn}₂)(MeCN)]PF₆ (**1**) complex (Scheme 1).

Scheme 1 Dehydrogenation of benzylamine with **1**.



RESULTS AND DISCUSSION

Benzylamine (BnNH₂) was chosen as the benchmark substrate that has three possible dehydrogenation products **A-C** (Scheme 1). Imine **A** is formed following dehydrogenation of BnNH₂ and coupling with a second substrate molecule (also called transamination), nitrile **B** is formed through two successive dehydrogenations, and dibenzylamine **C** forms through hydrogenation of imine **A** (termed hydrogen borrowing¹⁰). Catalysis with **1** (3 mol%) was evaluated at 110 °C in a variety of solvents (Table 1). Insolubility of **1** limited performance in toluene, a common solvent for other^{2a-d} AD catalysts (Entry 1). Polar solvents DMF and DMA give improved solubility and consumption of BnNH₂, but AD products are not observed and a control reaction without **1** likewise results in the consumption of BnNH₂. The dominant reactivity is ascribed to a competitive, uncatalyzed, coupling with the solvent (Entries 2-3). Other high-boiling polar solvents affords improved product formation (Entries 4-6) with the sustainable¹¹ solvent anisole giving the best performance. A conversion of 75% is achieved after 2 days and nearly complete consumption of BnNH₂ is reached after 4 days. This performance is similar to known catalysts^{2a-c} that reach maximum conversion with similar catalyst loadings (1-5 mol%) and shorter times (ca. 24 h), but at higher temperatures (115-150 °C). The products generated with **1** are imine **A** and nitrile **B** in a ca. 3:1 ratio, which is distinct from most reported catalysts that commonly^{10, 12} form hydrogen borrowing product **C**, though catalysts for selective production of **A** or **B** are known.^{2a-c, 2i} Release of the generated H₂ under a flow of N₂ does not lead to improved conversion or product selectivity. Treatment of **1** with amine **C** gives poor conversion suggesting secondary amines are challenging substrates (Entry 8). Addition of mercury does not negatively impact catalyst activity (Entry 9), supporting the homogeneity of the dehydrogenation catalyst.

The non-cooperative complex [Ru(Cp)(dppp)(MeCN)]PF₆, **2** is also catalytically active toward dehydrogenation of BnNH₂ (Entry 10; dppp = 1,3-

bis(diphenylphosphino)propane). Despite the absence of an internal base in the ligand backbone, **2** shows very good conversion (91%) under the optimized conditions. Again the major product is imine **A**, but both nitrile **B** and secondary amine **C** are observed as minor products. Thus an internal base is not required, suggesting that in the case of **2** the substrate acts as a suitable intermolecular base. Indeed, addition of NEt_3 as an exogenous base for catalyst **2** had no impact on the performance (Entry 11).

Table 1 – Catalytic optimization for the acceptorless dehydrogenation of benzylamine.^[a]

| Entry | [Ru] | Solvent ^[b] | Conv. (%) ^[c] | A (%) | B (%) | C (%) |
|-------------------|----------|------------------------|--------------------------|-------|-------|-------|
| 1 | 1 | Toluene | 7 | 6 | 0 | 0 |
| 2 | 1 | DMF | 99 | 2 | 0 | 0 |
| 3 | 1 | DMA | 71 | 19 | 17 | 1 |
| 4 | 1 | THFA | 32 | 22 | 10 | 1 |
| 5 | 1 | 2,4,6-collidine | 64 | 44 | 3 | 0 |
| 6 | 1 | Anisole | 76 | 54 | 20 | 3 |
| 7 ^[d] | 1 | Anisole | 95 | 69 | 18 | 8 |
| 8 ^[e] | 1 | Anisole | 18 | 1 | 0 | – |
| 9 ^[f] | 1 | Anisole | 94 | 34 | 50 | 0 |
| 10 | 2 | Anisole | 91 | 65 | 18 | 10 |
| 11 ^[g] | 2 | Anisole | 87 | 52 | 18 | 10 |

^[a] Conditions: 250 mM BnNH_2 , 3 mol% [Ru], 110 °C, 48 h, in a sealed vial. Quantification was conducted by calibrated GC-FID using an internal standard and values are an average of two runs and errors are $\leq \pm 5\%$. ^[b] DMF = dimethylformamide; DMA = dimethylacetamide; THFA = tetrahydrofurfuryl alcohol. ^[c] Amount of BnNH_2 consumed. ^[d] 96 h. ^[e] Substrate is **C**. ^[f] 100 μL of elemental mercury was added. ^[g] 15 mol% NEt_3 .

To further probe the scope and distinction between the $\text{P}^{\text{Ph}}_2\text{N}^{\text{Bn}}_2$ (**1**) and dppp (**2**) catalysts, AD of benzylamine was conducted in the presence of para-substituted anilines, R-ArNH_2 , to give coupled products **D** (Scheme 2). In all cases, the major product with **1** or **2** after 24 h is the homo-coupled product **A** (Figure 1 and S.I.). At this time in all cases, >75% consumption of BnNH_2 is observed and the amount of heterocoupled product **D** is <10%. Formation of **D** at longer reaction times (vide infra) likely proceeds following nucleophilic attack of the aniline on **A**, rather than on the primary imine (PhHC=NH) generated after AD of BnNH_2 . A comparison of product yields at 48 h reveals distinct selectivity for the two catalysts **1** and **2** (Table 2). With the MeO-ArNH_2 substrate, catalyst **1** gives the aniline coupled ADC product **D** as the major species with minor amounts of **A** and nitrile **B** (Figure 1a; Table 2, Entry 1). Comparison to reaction of **1** with BnNH_2 alone (Table 1, Entry 6) shows a similar distribution of dehydrogenation products **B** and **C**. The role of the aniline is predominantly as a nucleophile to convert the homocoupled product **A** to heterocoupled product **D**. In contrast, catalyst **2** gives only ca. 10% of **D** (Figure 1b; Table 2, Entry 2). While the aniline shows minimal participation as a nucleophile, it dramatically alters the product distribution as compared to ADC with BnNH_2 alone (Table 1, Entry 10). The Bronsted basicity of MeO-ArNH_2 diverts the selectivity of **2** from ADC product **A** to hydrogen borrowing product **C**.

Scheme 2 Acceptorless dehydrogenative coupling of benzylamine with anilines catalyzed by **1 or **2**.**

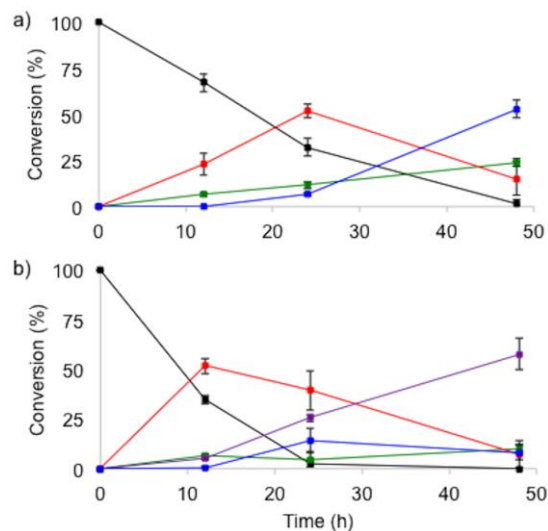
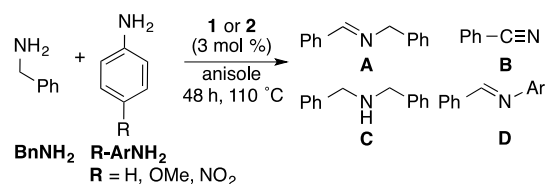


Figure 2. Conversion curves for the ADC of BnNH_2 (black) with MeO-ArNH_2 under the optimized conditions with catalyst a) **1**; and b) **2**. Yields, determined by calibrated GC-FID analysis, of reaction products **A** (red), **B** (green), **C** (purple) and **D** (blue) are plotted. Data points represent the average of the two runs and the error bars give the span of the conversion values of each data set.

With the less nucleophilic aniline H-ArNH_2 an unselective mixture of products is observed for both catalysts **1** and **2** (Table 2, Entries 3-4). Notably, the dppp catalyst **2** gives only minor amounts of hydrogen borrowing product **C**, but the aniline coupling product **D** is generated as a major product (along with nitrile **B**). This increase in **D** despite the lower nucleophilicity of the aniline relative to MeO-ArNH_2 is attributed to the lower Bronsted basicity of H-ArNH_2 . The $\text{P}^{\text{Ph}}_2\text{N}^{\text{Bn}}_2$ catalyst **1** mediates ADC in the presence of BnNH_2 and H-ArNH_2 to give **A** as the dominant product. This difference in selectivity relative to the reaction with MeO-ArNH_2 is expected based on the lower nucleophilicity of H-ArNH_2 , which decreases the yield of **D**. While proton shuttling by the aniline cannot be excluded for catalyst **1**, it should be noted that the participation of an external base does not necessarily preclude a cooperative mechanism for the $\text{P}^{\text{Ph}}_2\text{N}^{\text{Bn}}_2$ catalyst. Extensive mechanistic studies of $[\text{Ni}(\text{P}^{\text{R}}_2\text{N}^{\text{R}'}_2)_2]^{2+}$ electrocatalysts reveals that a pKa matched external base dramatically improves catalyst performance by shuttling protons to the correctly positioned pendent amine.¹³ ADC with $\text{NO}_2\text{-ArNH}_2$ does not give any of the heterocoupled product **D** with either catalyst **1** or **2** (Table 2, Entries 5-6). The electron-withdrawing nitro moiety decreases the nucleophilicity of the aniline sufficiently to inhibit coupling. The $\text{P}^{\text{Ph}}_2\text{N}^{\text{Bn}}_2$ catalyst gives **A** and **B** in a higher yield, but similar ratio (ca. 2.3:1; Table 2 Entry 5) to that observed without the aniline present (cf. 3:1; Table 1, Entry 6). Catalyst **2** also has similar conversion, but ca. 15% higher yield of the hydrogen borrowing product **C** is found (Table 2,

Entry 6) relative to reaction without the aniline (Table 1, Entry 10). Overall, the added aniline substrates alter the dehydrogenation selectivity with both the $P^{Ph_2}N^{Bn_2}$ (**1**) and dppp (**2**) catalysts. The Bronsted basicity of the aniline is a dominant indicator of selectivity for **2**, while the nucleophilic character most important for **1**.

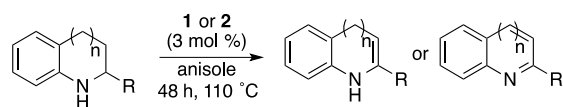
Table 2 – Catalytic acceptorless dehydrogenation of benzylamine with aniline derivatives R-ArNH₂.^[a]

| Entry | R ^[b] | [Ru] | Conv. (%) | A (%) | B (%) | C (%) | D (%) |
|-------|------------------|----------|-----------|-------|-------|-------|-------|
| 1 | OMe | 1 | 98 | 15 | 24 | 0 | 53 |
| 2 | | 2 | 100 | 7 | 10 | 58 | 8 |
| 3 | H | 1 | 98 | 42 | 38 | 0 | 19 |
| 4 | | 2 | 100 | 23 | 34 | 8 | 34 |
| 5 | NO ₂ | 1 | 98 | 73 | 32 | 0 | 0 |
| 6 | | 2 | 100 | 48 | 24 | 24 | 0 |

^[a] Conditions: 250 mM **BnNH₂**, 250 mM **R-ArNH₂**, 3 mol% **[Ru]**, 110 °C, 48 h, in a sealed vial. Quantification was conducted by calibrated GC-FID using an internal standard and values are an average of two runs and errors are <±5%, conversion curves are included in the S.I. ^[b] **R** of aniline substrates **R-ArNH₂**.

Complexes **1** and **2** are also competent catalysts for the acceptorless dehydrogenation of 5- and 6-membered heterocycles to give indole and quinoline products (Scheme 3, Table 3). Both catalysts dehydrogenate ca. 90% indoline (**Ind**) under the optimized catalytic conditions (Entries 1-2), with a faster rate than observed for **1** (see S.I. for conversion curves). By comparison, hydride catalysts RuH₂CO(PPh₃)₃, RuH₂(PPh₃)₃ and the Shvo catalyst each give >90% conversion of **Ind** to indole at a higher catalyst loading (5 mol%) and higher temperature (165 °C).^{2g} Similar performance is also found for RuCl₂(PPh₃)₃ at conditions (2 mol% and 110 °C) that are closer to those used for **1** and **2**.¹⁴ These prior studies and the results presented here show little distinction in catalyst performance in the AD of **Ind** between established cooperative (i.e. **1** and the Shvo catalysts) and non-cooperative catalysts. However, the $P^{Ph_2}N^{Bn_2}$ catalyst **1** outperforms dppp catalyst **2** in the dehydrogenation of **Me-Ind** to give 2-methylindole (Table 3, Entries 3-4). This suggests **1** is more tolerant of steric bulk at the site of dehydrogenation than **2**. Both catalysts show poor performance in the AD of the 6-membered heterocycle 1,2,3,4-tetrahydroquinoline (**THQ**; Entries 5-6).

Scheme 3 Acceptorless dehydrogenation of *N*-heterocycles^[a] by **1** or **2**.

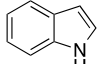
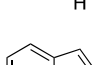
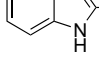
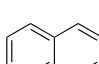
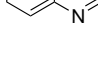
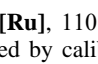


^[a] Indoline (**Ind**), R = H, n = 0; 2-methylindoline (**Me-Ind**), R = Me, n = 0; 1,2,3,4-tetrahydroquinoline (**THQ**), R = H, n = 1.

The different overall activity and selectivity of $P^{Ph_2}N^{Bn_2}$ catalyst **1** and dppp catalyst **2** led us to question the role of the pendent amine of **1** in the dehydrogenation mechanism. Stoichiometric reactions of **1** were thus conducted to identify potential catalytic intermediates (Scheme 4). Treatment of **1** with 5 equiv. benzylamine at 65 °C does not give catalytic

turnover, but a new product is formed as judged by the ca. 10 ppm upfield shift of the $^{31}P\{^1H\}$ NMR signal. In a larger-scale reaction, the product is isolated (85% yield) and is identified as amine-adduct **3** (Scheme 2a). Benzylamine coordination is supported by MALDI mass spectrometry that gives a signal with an isotope pattern and *m/z* value (757.2) that match to simulated values for $[3-PF_6+H]^+$. The new methylene and aryl signals in the 1H NMR spectrum overlap with existing signals, but their presence is evident by a change in integration. The signal for the amine Ru-NH₂Bn moiety is observed at 4.91 ppm, which is ca. 1 ppm downfield as compared to other $[Ru]-NH_2Bn$ complexes.¹⁵ We hypothesize that the downfield shift may be due to a hydrogen-bonding interaction between the N-H moiety of the benzylamine ligand and the pendent tertiary amine of the $P^{Ph_2}N^{Bn_2}$ ligand. Identification of through space interactions from the N-H signal to the methylene of the $P^{Ph_2}N^{Bn_2}$ benzyl moiety by $^1H-^1H$ ROESY NMR analysis are inconclusive due to the overlap of the latter signal with the methylene of the benzylamine ligand.

Table 3 – Performance of 1 and 2 toward acceptorless dehydrogenation of *N*-heterocycles.^[a]

| Entry | Sub. | [Ru] | Conv. (%) | Prod. | Yield (%) |
|-------|---------------|----------|-----------|---|-----------|
| 1 | Ind | 1 | 94 |  | 88 |
| 2 | Ind | 2 | 91 |  | 91 |
| 3 | Me-Ind | 1 | 93 |  | 78 |
| 4 | Me-Ind | 2 | 68 |  | 54 |
| 5 | THQ | 1 | 20 |  | 11 |
| 6 | THQ | 2 | 27 |  | 24 |

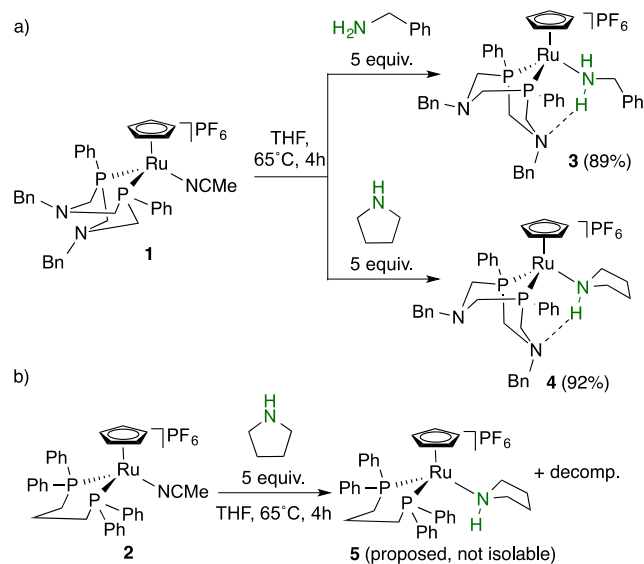
^[a] Conditions: 250 mM Sub., 3 mol% **[Ru]**, 110 °C, 48 h, in a sealed vial. Quantification was conducted by calibrated GC-FID using an internal standard and values are an average of two runs and errors are <±5%, conversion curves are included in the S.I.

Compound **4**, the pyrrolidine analogue of **3**, was synthesized to evaluate the potential for hydrogen bonding between the metal-bound amine and the pendent amine of the $P^{Ph_2}N^{Bn_2}$ ligand (Scheme 4a). At the lower temperature used for the synthesis of **4** (65 °C) relative to catalysis (110 °C), no evidence of dehydrogenated pyrrolidine was observed. $^1H-^1H$ ROESY analysis of **4** reveals two notable correlations between one of the $P^{Ph_2}N^{Bn_2}$ N-Bn substituents and the pyrrolidine ligand: 1) H_s to H_j; and 2) H_i to H_v (Figure 2a). These suggest that, in the solution-state, the pendent amine is positioned close to the bound pyrrolidine. By contrast, no correlation is found between the $P^{Ph_2}N^{Bn_2}$ N-Bn methylene and the methyl protons of the acetonitrile ligand in **1**. The location of the NH signal for **4** (6.30 ppm) is shifted significantly downfield relative to related Ru(II)-amine complexes (ca. 3-4 ppm)^{15a, 16} and further supports the presence of a hydrogen-bond in solution.

Single crystals of **4** were successfully obtained and the aforementioned intramolecular hydrogen-bonding interaction is evident from the solid-state structure (Figure 2b). The N1-N3 distance of 2.953(7) Å is in the expected range for similar intramolecular N-N hydrogen-bonding distances (2.7 – 3.0 Å).¹⁷ The proximal six-membered metallocycle of the $P^{Ph_2}N^{Bn_2}$ ligand is in a boat conformation, pointing toward the pyrroli-

dine ligand. By comparison, the metallocyclic ring in all crystallized $\text{Ru}(\text{Cp}/\text{Cp}^*)(\text{P}^{\text{R}_2}\text{N}^{\text{R}_2})(\text{L})$ complexes is in a chair conformation with the pendent base pointed away from ligand L ($\text{X} = \text{MeCN}, \text{Cl}, \text{O}_2$), unless the amine is protonated and hydrogen bonds to L (i.e. $\text{N-H}\cdots\text{O}_2$).^{9, 18}

Scheme 4. Reactivity of: a) 1 with benzylamine or pyrrolidine; and b) 2 with pyrrolidine.



Attempts to synthesize a pyrrolidine adduct with dppp complex **2** also afforded a new product tentatively assigned as **5** in a 27% yield after 4 h as judged by $^{31}\text{P}\{^1\text{H}\}$ NMR spectroscopy (Scheme 4b). The product is unstable to isolation and it is accompanied by significant decomposition as is evidenced by formation of solids and a loss of ^{31}P integration over time. This is further support that a hydrogen bond is a stabilizing force in amine adducts **3** and **4**.

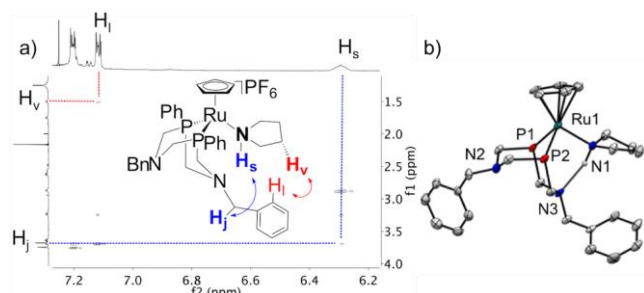
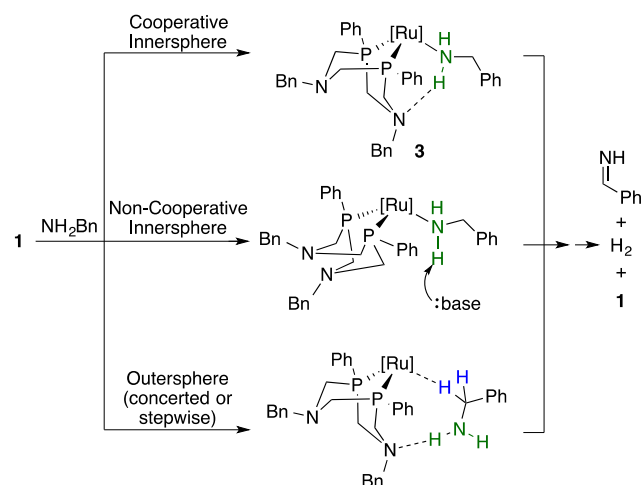


Figure 2. a) Expanded section of the ^1H - ^1H ROESY NMR spectrum of **4**; and b) Thermal displacement plot of **4** (right) with ellipsoids at 50% probability. Phenyl groups on P1 and P2 and the PF_6^- anion were removed for clarity.

The catalytic mechanism for **1** could follow one of three possible general paths: cooperative innersphere; non-cooperative inner-sphere or cooperative outersphere (Scheme 5). Amine coordination, to give the isolated compound **3**, is the first step in either a cooperative or non-cooperative inner-sphere pathway. The cooperative route would involve substrate deprotonation by the pendent base and β -H elimination from the bound amido. These steps would give a Ru-H that would be protonated by the pendent group to release H_2 . In such a route complex **3** would be an on-cycle catalytic species and a precursor to deprotonation. Thus it should have the

same, or higher, activity toward amine dehydrogenation as compared to precatalyst **1** that must dissociate MeCN prior to entering the cycle. The non-cooperative route is similar, except an exogenous base (i.e. a second equivalent of substrate) deprotonates the bound substrate and shuttles the proton back to the hydride. Finally, proton and hydride can be transferred to the catalyst through an outersphere route (either concerted or stepwise) without coordination of the amine nitrogen to the metal centre.

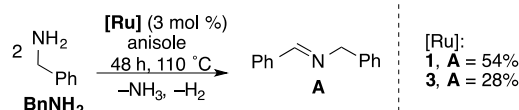
Scheme 5. Possible pathways for the dehydrogenation of benzylamine with catalyst 1.^[a]



^[a] $[\text{Ru}] = [\text{Ru}(\text{Cp})]\text{PF}_6$

Catalytic testing of **3** under the optimized conditions revealed that the amine adduct has significantly lower activity than **1**, with only 28% imine formed over 48 h (Scheme 6; see S.I. for conversion curve). This suggests that the benzylamine adduct **3** is not an on-cycle intermediate and that dehydrogenation does not proceed through an inner-sphere cooperative mechanism. Instead, **3** is an off-cycle species that enters the catalytic cycle by amine dissociation to follow a cooperative outersphere pathway or by cleavage of the hydrogen bond to follow a non-cooperative mechanism, which would be operative for the dppp catalyst **2**.

Scheme 6. Catalytic performance comparison of precatalysts 1 and benzylamine adduct 3 toward AD of benzylamine.



CONCLUSIONS

The complex $[\text{Ru}(\text{Cp})(\text{P}^{\text{Ph}_2}\text{N}^{\text{Bn}_2})(\text{NCMe})]\text{PF}_6$ (**1**) is an active acceptorless dehydrogenation catalyst toward benzylamine and it preferentially forms imine and nitrile products. The related complex $[\text{Ru}(\text{Cp})(\text{dppp})(\text{NCMe})]\text{PF}_6$ (**2**) shows competitive activity, but selectivity favours the hydrogen borrowing product (Bn_2NH). Both catalysts show similar activity, but different selectivity, toward AD of benzylamine and coupling with various anilines. They are both competitive catalysts for the dehydrogenation of 5-membered *N*-heterocycles. This comparison of the cooperative $\text{P}^{\text{Ph}_2}\text{N}^{\text{Bn}_2}$ and non-cooperative dppp ligands reveals that product selectivity is the dominant

difference between the catalysts. While the dppp catalyst must follow a non-cooperative pathway, the mode of action of the pendent amine in **2** is less obvious. Isolation and characterization of Ru-benzylamine and Ru-pyrrolidine adducts (**3** and **4**, respectively) reveals that these species are stabilized by a hydrogen bond formed with the $P^{Ph_2}N^{Bn_2}$ ligand. Poor catalytic performance of the benzylamine adduct **3** indicates that it is not a precursor to substrate deprotonation and is not an on-cycle catalyst intermediate. This study excludes an inner-sphere cooperative mechanism for **1**, leaving an outer-sphere cooperative or non-cooperative mechanisms as possible routes. Since the aniline basicity in ADC reactions with **1** has minimal impact on the dehydrogenation selectivity (only the subsequent coupling), a non-cooperative (base assisted) route is less likely for the $P^{Ph_2}N^{Bn_2}$ catalyst. Elucidation of the dominant pathway in acceptorless dehydrogenation with **1** will be investigated in due course.

EXPERIMENTAL SECTION

General Considerations. All reactions were manipulated under N_2 using standard Schlenk or glovebox techniques unless otherwise stated. All glassware was oven dried prior to use. Benzylamine (>98%), triphenylphosphine oxide (99%), aniline (>99%) and 2,4,6-collidine (99%) were obtained from Alfa Aesar. Pyrrolidine (>99%) was obtained from Fluka. NEt_3 (99%) was obtained from Caledon Laboratory Chemicals. Pyrene (98%), anisole (99%), dimethylacetamide (99%) and tetrahydrofurfuryl alcohol (THFA) (99%) were obtained from Sigma-Aldrich. *p*-Anisidine (99%) and *p*-nitroaniline (99%) were obtained from Oakwood Chemicals. Chloroform-*d* (99.8%) was obtained from Cambridge Isotope Laboratories. $[Ru(Cp)(P^{Ph_2}N^{Bn_2})(NCMe)]PF_6$ (**1**) and $[Ru(Cp)(dppp)(NCMe)]PF_6$ (**2**) were synthesized following literature procedures.⁹ Dry and degassed tetrahydrofuran (THF), toluene, dichloromethane (DCM), hexanes, dimethylformamide (DMF), dioxane and acetonitrile (MeCN) were obtained from an Innovative Technology 400-5 Solvent Purification System and stored under N_2 . These dry and degassed solvents, except for MeCN, were stored over 4 Å molecular sieves (Fluka and activated at 150 °C for over 12 h). Triethylamine was dried with 4 Å molecular sieves and degassed by bubbling with N_2 . Chloroform-*d* was dried with 4 Å molecular sieves and degassed by bubbling with N_2 . Benzylamine was dried with NaOH, distilled under vacuum and stored under N_2 . All other chemicals were used as obtained.

Charge-transfer Matrix Assisted Laser Desorption/Ionization mass spectrometry (MALDI) data were collected on an AB Sciex 5800 TOF/TOF mass spectrometer using pyrene as the matrix in a 20:1 molar ratio to complex. Solutions were prepared in DCM and spotted on a sample plate under an inert atmosphere and transferred to the instrument in a sealed Ziplock® bag. The instrument is equipped with a 349 nm OptiBeam On-Axis laser. The laser pulse rate was 400 Hz and data were collected in reflectron positive mode. Reflectron mode was externally calibrated at 50 ppm mass tolerance. Each mass spectrum was collected as a sum of 500 shots. All NMR spectra were recorded on either an Inova 400 or 600 MHz, or Mercury 400 MHz instrument. 1H and ^{13}C spectra acquired in $CDCl_3$ were referenced internally against residual solvent signals ($CHCl_3$) to TMS at 0 ppm. ^{31}P spectra were referenced externally to 85% phosphoric acid at 0.00 ppm. Infrared spectra were collected on a PerkinElmer UATR TWO FTIR spectrometer. Elemental analysis was performed by Laboratoire d'Analyse Élémentaire de l'Université de Montréal. Quantification of catalytic reactivity was achieved using an Agilent 7890a gas chromatograph with a flame ionization detector (GC-FID). A HP-5 column was used. Benzylamine, phenyl-*N*-(phenylmethyl)-methanimine, dibenzylamine, and benzonitrile were calibrated relative to the internal standard (tetrahydronaphthlene).

Synthesis of $[Ru(Cp)(P^{Ph_2}N^{Bn_2})(benzylamine)]PF_6$ (3**).** $[Ru(Cp)(P^{Ph_2}N^{Bn_2})(NCMe)]PF_6$ (**1**) (101 mg, 0.121 mmol, 1 equiv.) was added to a 100 mL Schlenk flask with a stir bar in the glovebox.

Dry THF (10 mL) and $BnNH_2$ (13 μ L, 0.12 mmol, 1 equiv.) were added by micropipette and micro syringe, respectively. The Schlenk flask was fitted with a condenser and heated to reflux on the Schlenk line for 4 h. The solvent was removed under vacuum to afford a brown powder that was washed with Et_2O . Yield: 98 mg (89%). 1H (600 MHz, $CDCl_3$): δ 7.64-7.59 (m, Ph-*H*, 4H), 7.55-7.48 (m, Ph-*H*, 6H), 7.36-7.28 (m, Ph-*H*, 6H), 7.25-7.17 (m, Ph-*H*, 3H), 7.14-7.09 (m, Ph-*H*, 2H), 7.08-7.03 (m, Ph-*H*, 2H), 6.94-6.88 (m, Ph-*H*, 2H), 4.91 (broad, $BnNH_2$, 2H), 4.73 (s, Cp-*H*, 5H), 3.66-3.60 (m, NCH_2P , NCH_2Ph , $RuNH_2CH_2Ph$, 8H), 3.47 (s, NCH_2Ph , 2H), 3.09 (m, NCH_2P , 2H), 2.47 (m, NCH_2P , 2H). $^{31}P\{^1H\}$ (243 MHz, $CDCl_3$): δ 29.2 (s, RuP), -144.3 (sept, $^1J_{P-F}$ = 715 Hz, PF_6^-). $^{13}C\{^1H\}$ (151.5 MHz, $CDCl_3$): δ 139.7 (Ph-*C* ring), 136.5 (Ph-*C* ring), 134.2 (Ph-*C* ring), 134.1 (Ph-*C* ring), 131.4 (Ph-*C* ring), 131.2 (Ph-*C* ring), 130.0 (Ph-*C* ring), 129.6 (Ph-*C* ring), 129.1-128.5 (Ph-*C* ring), 128.4-127.9 (Ph-*C* ring), 81.1 (s, *Cp*), 67.4 (s, NCH_2Ph) and 64.7 (s, NCH_2Ph), 60.1 (s, NH_2CH_2Ph), 58.3 (s, NCH_2P) and 55.2 (s, NCH_2P). MALDI MS (pyrene matrix): Calc. m/z 757.2 [**3** - PF_6^- + H^+], Obs. m/z 757.2. A crystalline sample was obtained following vapor diffusion of Et_2O into a concentrated solution of **3** in acetone. Anal. Calc. for $C_{42}H_{46}F_6N_3P_3Ru$: C, 56.00; H, 5.15; N, 4.66. Found: C, 56.47; H, 5.25; N, 4.62.

Synthesis of $[Ru(Cp)(P^{Ph_2}N^{Bn_2})(pyrrolidine)]PF_6$ (4**).** $[Ru(Cp)(P^{Ph_2}N^{Bn_2})(NCMe)]PF_6$ (**1**) (150 mg, 0.180 mmol, 1 equiv.) was added to a 100 mL Schlenk flask with a stir bar. Dry THF (10 mL) and pyrrolidine (60 μ L, 0.90 mmol, 5 equiv.) were added by micropipette and micro syringe, respectively. The reaction was heated to reflux on the Schlenk line for 4 h. The solvent was removed under vacuum to afford a brown product that was washed with Et_2O . Yield: 142 mg (92%). Purity = 90% by NMR. Single crystals were formed following vapor diffusion of Et_2O into a concentrated solution of product in acetone. Upon dissolving single crystals of **4** in THF or $CDCl_3$, ca. 10% decomposition is observed by 1H and ^{31}P NMR spectroscopy in 10–15 min, after which no further decomposition is observed. 1H (600 MHz, $CDCl_3$): δ 7.62 (m, H_a , 4H), 7.53-7.47 (m, H_b , H_c , 6H), 7.36-7.30 (m, H_m , H_n , H_r , H_q , 6H), 7.21 (m, H_i , 2H), 7.13 (m, H_p , 2H), 6.30 (broad, H_s , 1H), 4.72 (s, Cp-*H*, 5H), 3.76 (s, H_i , 2H), 3.71 (m, N- CH_g -P, 2H), 3.70 (s, H_j , 2H), 3.65 (m, N- CH_e -P, 2H), 3.23 (m, N- CH_g -P, 2H), 2.88 (m, H_i , 2H), 2.63 (m, N- CH_f -P, 2H), 2.58 (m, H_u , 2H), 1.76 (m, H_w , 2H), 1.51 (m, H_v , 2H). $^{31}P\{^1H\}$ (243 MHz, $CDCl_3$): δ 29.3 (s, *P*-Ph), -144.3 (sept, $^1J_{P-F}$ = 713 Hz, PF_6^-). $^{13}C\{^1H\}$ (151.5 MHz, $CDCl_3$): δ 136.8 (s, C_o), 135.2 (s, C_k), 134.0 (dd, $^1J_{C-P}$ = 19.9 Hz, $^3J_{C-P}$ = 19.9 Hz, C_d), 131.3 (m, C_a), 129.9 (s, C_c , C_l , C_p), 126.6 (m, C_b), 129.1 (s, C_q), 129.0 (s, C_m), 128.5 (s, C_r), 128.1 (s, C_n), 81.6 (s, C_p), 66.4 (s, C_j), 65.4 (s, C_i), 62.4 (s, C_i), 58.5 (dd, $^1J_{C-P}$ = 26.3 Hz, $^3J_{C-P}$ = 26.3 Hz, C_e), 55.8 (dd', $^1J_{C-P}$ = 17.7 Hz, $^3J_{C-P}$ = 17.7 Hz, C_g), 26.1 (s, C_w). MALDI MS (anthracene matrix): Calc. m/z 717.2 [**4** - PF_6^- - 3 H^+], Obs. m/z 717.2. Anal. Calc. for $C_{39}H_{46}F_6N_3P_3Ru$: C, 54.17; H, 5.36; N, 4.86. Found for a crystalline sample: C, 54.61; H, 5.43; N, 4.77.

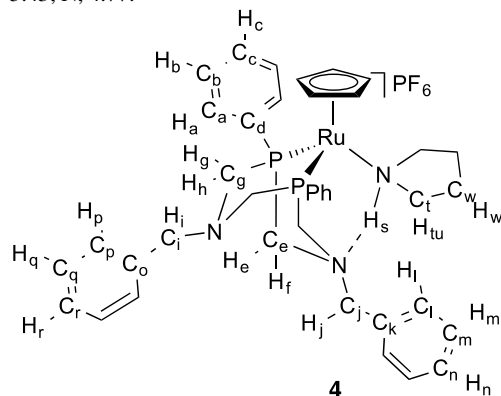


Figure 2. Numbering scheme for 1H and ^{13}C NMR assignment for complex **4**.

General Procedure for Catalytic Dehydrogenation Reactions of Benzylamine. In a glovebox, the following stock solutions were prepared: Benzylamine (322 mg, 3.00 mmol, 1 M) and tetrahydronaphthalene (159 mg, 1.20 mmol, 400 mM) in anisole (3.00 mL); **1** (7.5 mg, 0.011 mmol, 15 mM) in anisole (0.750 mL); **2** (14 mg, 0.019 mmol, 15 mM) in anisole (1.250 mL). Four sets, A-D, of 2 vials (8 vials total) containing stir bars were charged with the benzylamine stock solution (125 μ L). To each of these vials the catalyst stock **1** (250 μ L to set A), and **2** (250 μ L to set B and C) along with additional anisole solvent (125 μ L for A-C, 375 μ L for D) were added. Triethylamine (1.1 μ L, 0.76 mmol) was added to each vial in set C. The final concentrations for vials in sets A-D were 0.25 M in benzyl amine with 3 mol% catalyst loading (A-C), and set D contained no catalyst. A final vial was charged with substrate/internal standard stock solution (100 μ L) for use as the initial time = 0 (T0) sample for GC-FID analysis. The vials (except T0 sample) were capped and removed from the glove box and heated to 110 °C with stirring. After 24 and 48 hours one vial from each of the sets was removed from heat, cooled, and exposed to air to quench. An aliquot (40 μ L) was diluted to 10 mM benzylamine with MeCN (960 μ L) and analyzed by GC-FID. A 20 μ L aliquot of the T0 sample was diluted with solvent (980 μ L) and analyzed by GC-FID.

General Procedure for Catalytic Dehydrogenation Reactions of Benzylamine with Anilines. In a glovebox, the following stock solutions were prepared: Benzylamine (322 mg, 3.00 mmol, 1 M) and tetrahydronaphthalene (159 mg, 1.20 mmol, 400 mM) in anisole (3.00 mL); aniline (279 mg, 3 mmol, 1M) in anisole (3.00 mL); **1** (15 mg, 0.22 mmol, 15 mM) in anisole (1.50 mL); **2** (17 mg, 0.022 mmol, 15 mM) in anisole (1.500 mL). Benzylamine and aniline stock solutions were combined (500 mM). Two sets, A-B, of 3 vials (6 vials total) containing stir bars were charged with the benzylamine/aniline stock solution (250 μ L). To each of these vials the catalyst stock **1** (250 μ L to set A), and **2** (250 μ L) to set B. The final concentrations for vials in sets A-B were 0.25 M in benzyl amine with 3 mol% catalyst loading (A-B). A final vial was charged with substrate/internal standard stock solution (100 μ L) for use as the initial time = 0 (T0) sample for GC-FID analysis. The vials (except T0 sample) were capped and removed from the glove box and heated to 110 °C with stirring. After 12, 24 and 48 hours one vial from each of the sets was removed from heat, cooled, and exposed to air to quench. An aliquot (40 μ L) was diluted to 10 mM benzylamine with MeCN (960 μ L) and analyzed by GC-FID. A 20 μ L aliquot of the T0 sample was diluted with solvent (980 μ L) and analyzed by GC-FID.

General Procedure for Catalytic Dehydrogenation Reactions of N-Heterocycles. In a glovebox, the following stock solutions were prepared: Indoline (357 mg, 3.00 mmol, 500 mM) and tetrahydronaphthalene (80 mg, 0.60 mmol, 200 mM) in anisole (6.00 mL); **1** (15 mg, 0.022 mmol, 15 mM) in anisole (1.500 mL); **2** (17 mg, 0.022 mmol, 15 mM) in anisole (1.500 mL). Two sets, A-B, of 5 vials (10 vials total) containing stir bars were charged with the indoline stock solution (250 μ L). To each of these vials the catalyst stock **1** (250 μ L to set A), and **2** (250 μ L) to set B. The final concentrations for vials in sets A-B were 0.25 M in indoline with 3 mol% catalyst loading (A-B). A final vial was charged with substrate/internal standard stock solution (100 μ L) for use as the initial time = 0 (T0) sample for GC-FID analysis. The vials (except T0 sample) were capped and removed from the glove box and heated to 110 °C with stirring. After 1, 4, 12, 24 and 48 hours one vial from each of the sets was removed from heat, cooled, and exposed to air to quench. An aliquot (200 μ L) was diluted to 50 mM indoline with MeCN (800 μ L) and analyzed by GC-FID. A 100 μ L aliquot of the T0 sample was diluted with solvent (900 μ L) and analyzed by GC-FID.

General Procedure for Stoichiometric Probe Reactions with [Ru(Cp)(dppp)(NCMe)]PF₆ (2**).** Complex **2** (8 mg, 0.01 mmol, 1 equiv.) and triphenylphosphine oxide (3 mg, 0.01 mmol, 1 equiv.) were added to a vial with a stir bar. THF (0.800 mL) was added by micropipette. The solution was transferred to a NMR tube and an initial (time = 0) ³¹P{¹H} NMR spectrum was obtained. The tube contents were transferred back to the vial containing the stir bar and substrate (benzylamine or pyrrolidine) (0.5 mmol, 5 equiv.) was added. The vial was stirred and heated to 65 °C in an aluminum heating

block for 4 h. The contents were transferred back into a clean NMR tube and a ³¹P{¹H} NMR spectrum was obtained. If more time points were obtained, the process of heating in the vial and transfer to NMR tube were repeated for each subsequent time point.

Attempted synthesis of [Ru(Cp)(dppp)(pyrrolidine)]PF₆ (5**).** Complex **2** (77 mg, 0.1 mmol, 1 equiv.) was added to a 100 mL Schlenk flask with a stir bar and THF (8 mL) was added. To the Schlenk flask, pyrrolidine (36 mg, 0.5 mmol, 5 equiv.) was added. The Schlenk flask was stirred and heated to 65 °C for 45 h. The reaction was monitored over time until all of complex **2** producing black particles. The solvent was removed under vacuum and the ³¹P{¹H} NMR spectra were obtained in either proteo-THF or CDCl₃ revealing full decomposition in both solvents.

ASSOCIATED CONTENT

Supporting Information

The Supporting Information is available free of charge on the ACS Publications website.

Spectral data, diffraction data and catalysis conversion graphs (PDF)

Single crystal diffraction data for **4** (CIF)

AUTHOR INFORMATION

Corresponding Author

* E-mail: johanna.blacquiere@uwo.ca

Notes

The authors declare no competing financial interests.

ACKNOWLEDGMENT

This work was financially supported by a Natural Sciences and Engineering Research Council (NSERC) of Canada Discovery Grant and The University of Western Ontario. JMS thanks the Ontario Graduate Scholarship program for funding.

REFERENCES

- (a) Gunanathan, C.; Milstein, D., *Chem. Rev.* **2014**, *114*, 12024-12087; (b) Gunanathan, C.; Milstein, D., *Acc. Chem. Res.* **2011**, *44*, 588-602.
- (a) Tseng, K.-N. T.; Rizzi, A. M.; Szymczak, N. K., *J. Am. Chem. Soc.* **2013**, *135*, 16352-16355; (b) He, L.-P.; Chen, T.; Gong, D.; Lai, Z.; Huang, K.-W., *Organometallics* **2012**, *31*, 5208-5211; (c) Prades, A.; Peris, E.; Albrecht, M., *Organometallics* **2011**, *30*, 1162-1167; (d) Ho, H.-A.; Manna, K.; Sadow, A. D., *Angew. Chem. Int. Ed.* **2012**, *51*, 8607-8610; (e) Fujita, K.-i.; Tanaka, Y.; Kobayashi, M.; Yamaguchi, R., *J. Am. Chem. Soc.* **2014**, *136*, 4829-4832; (f) Wu, J.; Talwar, D.; Johnston, S.; Yan, M.; Xiao, J., *Angew. Chem. Int. Ed.* **2013**, *52*, 6983-6987; (g) Muthaiah, S.; Hong, S. H., *Adv. Synth. Catal.* **2012**, *354*, 3045-3053; (h) Chakraborty, S.; Brennessel, W. W.; Jones, W. D., *J. Am. Chem. Soc.* **2014**, *136*, 8564-8567; (i) Myers, T. W.; Berben, L. A., *J. Am. Chem. Soc.* **2013**, *135*, 9988-9990.
- Largerion, M., *Eur. J. Org. Chem.* **2013**, *2013*, 5225-5235.
- Grellier, M.; Sabo-Etienne, S., *Dalton Trans.* **2014**, *43*, 6283-6286.
- Zell, T.; Milstein, D., *Acc. Chem. Res.* **2015**, *48*, 1979-1994.
- (a) Khusnutdinova, J. R.; Milstein, D., *Angew. Chem. Int. Ed.* **2015**, *54*, 12236-12273; (b) Crabtree, R. H., *New J. Chem.* **2011**, *35*, 18-23; (c) Grützmacher, H., *Angew. Chem. Int. Ed.* **2008**, *47*, 1814-1818.
- (a) Sun, Y.; Koehler, C.; Tan, R.; Annibale, V. T.; Song, D., *Chem. Commun.* **2011**, *47*, 8349-8351; (b) Zhang, J.; Leitius, G.; Ben-David, Y.; Milstein, D., *Angew. Chem. Int. Ed.* **2006**, *45*, 1113-1115; (c) Ben-Ari, E.; Leitius, G.; Shimon, L. J. W.; Milstein, D., *J.*

- Am. Chem. Soc.* **2006**, *128*, 15390-15391; (d) Hou, C.; Zhang, Z.; Zhao, C.; Ke, Z., *Inorg. Chem.* **2016**, *55*, 6539-6551; (e) Cho, D.; Ko, K. C.; Lee, J. Y., *Organometallics* **2013**, *32*, 4571-4576; (f) Yang, X.; Hall, M. B., *J. Am. Chem. Soc.* **2010**, *132*, 120-130.
8. (a) Bullock, R. M.; Helm, M. L., *Acc. Chem. Res.* **2015**, *48*, 2017-2026; (b) Bullock, R. M.; Appel, A. M.; Helm, M. L., *Chem. Commun.* **2014**, *50*, 3125-3143; (c) Liu, T.; DuBois, M. R.; DuBois, D. L.; Bullock, R. M., *Energy Environ. Sci.* **2014**, *7*, 3630-3639.
9. Stubbs, J. M.; Bow, J. P. J.; Hazlehurst, R. J.; Blacquiere, J. M., *Dalton Trans.* **2016**, *45*, 17100-17103.
10. Dobereiner, G. E.; Crabtree, R. H., *Chem. Rev.* **2010**, *110*, 681-703.
11. Alder, C. M.; Hayler, J. D.; Henderson, R. K.; Redman, A. M.; Shukla, L.; Shuster, L. E.; Sneddon, H. F., *Green Chem.* **2016**, *18*, 3879-3890.
12. Bui The, K.; Concilio, C.; Porzi, G., *J. Organomet. Chem.* **1981**, *208*, 249-251.
13. (a) Raugei, S.; Helm, M. L.; Hammes-Schiffer, S.; Appel, A. M.; O'Hagan, M.; Wiedner, E. S.; Bullock, R. M., *Inorg. Chem.* **2016**, *55*, 445-460; (b) O'Hagan, M.; Ho, M.-H.; Yang, J. Y.; Appel, A. M.; DuBois, M. R.; Raugei, S.; Shaw, W. J.; DuBois, D. L.; Bullock, R. M., *J. Am. Chem. Soc.* **2012**, *134*, 19409-19424.
14. Tsuji, Y.; Kotachi, S.; Huh, K. T.; Watanabe, Y., *J. Org. Chem.* **1990**, *55*, 580-584.
15. (a) Nyawade, E. A.; Friedrich, H. B.; Omondi, B.; Mpungose, P., *Organometallics* **2015**, *34*, 4922-4931; (b) Sortais, J.-B.; Pannetier, N.; Holuigue, A.; Barloy, L.; Sirlin, C.; Pfeffer, M.; Kyritsakas, N., *Organometallics* **2007**, *26*, 1856-1867.
16. (a) Lummiss, J. A. M.; Ireland, B. J.; Sommers, J. M.; Fogg, D. E., *ChemCatChem* **2014**, *6*, 459-463; (b) Fogg, D. E.; James, B. R., *Inorg. Chem.* **1995**, *34*, 2557-2561.
17. (a) Dabb, S. L.; Messerle, B. A.; Wagler, J., *Organometallics* **2008**, *27*, 4657-4665; (b) Prokopchuk, D. E.; Lough, A. J.; Morris, R. H., *Dalton Trans.* **2011**, *40*, 10603-10608.
18. (a) Tronic, T. A.; Kaminsky, W.; Coggins, M. K.; Mayer, J. M., *Inorg. Chem.* **2012**, *51*, 10916-10928; (b) Tronic, T. A.; Rakowski DuBois, M.; Kaminsky, W.; Coggins, M. K.; Liu, T.; Mayer, J. M., *Angew. Chem. Int. Ed.* **2011**, *50*, 10936-10939.

